



Structural context of the Flatreef in the Northern Limb of the Bushveld Complex

J. A. N. Brits¹ · D. F. Grobler¹ · A. Crossingham² · T. G. Blenkinsop³ · W. D. Maier³

Received: 11 January 2024 / Accepted: 1 June 2024
© The Author(s) 2024

Abstract

The Flatreef occurs at a depth of 700 m under the farm Turfspruit 241 KR in the Northern Limb of the Bushveld Complex. The Flatreef forms part of the Platreef of the Northern Limb, which contains magmatic rocks of the Rustenburg Layered Suite of the Bushveld Complex. The structure of the Flatreef is a flat-lying to gently westerly dipping monoclinical to open fold, 1 km wide and 6 km long. Distinctive features within the Flatreef include the development of cyclical magmatic layering with locally thickened pyroxenitic layers, and associated economically significant poly-metallic mineralisation. Geophysical evidence, exploration drill core, and recent underground exposure show that deformation had a major influence on the Flatreef mineralization. Block faulting and first generation folding affected the orientation and shape of the sedimentary host-rock sequence prior to intrusion of the Rustenburg Layered Suite. These structural and host-rock elements controlled the intrusion of the Lower Zone, and to a lesser degree, the Critical Zone correlatives of the Bushveld Complex in the Northern Limb. During intrusion reverse faults and shear zones and a second generation of folds were active, as well as local extension along layering. Syn-magmatic deformation on these structures led to laterally extensive stratal thickening across them, including the Merensky-Reef correlative that forms part of the Flatreef. This deformation was likely to have been driven by subsidence of the Bushveld complex. Many of these structures were intruded by granitic magmas during the late stages of intrusion, and they were reactivated during extension after intrusion. “Thus, structures were active before, during and after the intrusion of the Northern Limb, and the structural evolution determined the current geometry and mineral endowment of the Flatreef.”

Keywords Bushveld complex · Platinum · Structural geology · Northern limb · Flatreef · Syn-magmatic deformation

Introduction

The Bushveld Complex is the largest layered intrusion and ore belt on Earth, containing the world’s largest resource of platinum-group elements, vanadium, and chromium, as well as significant Ni and Cu (Willemse 1969; Mudd et al. 2018). The complex is exposed in three major limbs, namely the

Western, Eastern, and Northern Limbs. In the Western and Eastern limbs, PGE mineralisation occurs mainly in the form of relatively narrow (typically several dm) stratiform reefs, located in the Critical Zone, several km above the base of the intrusion (Lea 1996; Naldrett et al. 1986; Maier et al. 2013). In the Northern Limb, the bulk of the mineralisation also occurs in the Critical Zone, but here the Lower Zone is much thinner than in the other limbs so that the mineralisation is located near the base of the complex, as contact-style mineralisation (e.g. Maier et al. 2008). This is characterised by somewhat lower and more variable grade than the internal reefs, but much greater thickness than in the other limbs (10s of m) (McDonald and Holwell 2011). The Northern Limb hosts the largest mine of the Complex (the Mokgalakwena Pt mine) and is the focus of much current exploration and development activity.

The Flatreef mineralised zone is interpreted as the down-dip extension of the Platreef (Kekana 2014; Grobler et al. 2019; Maier et al. 2021, 2023). A recent stratigraphic

Editorial handling: E. Mansur.

✉ J. A. N. Brits
abrits@criticalminerals.com

¹ Ivanplats (Pty) Ltd, an Ivanhoe Mines Company, 82 on Maude, Second Floor, 82 Maude Street, Sandton 2146, South Africa

² Stillwater Critical Minerals Corporation, Suite 904 – 409 Granville Street, V6C 1T2 Vancouver, BC, Canada

³ School of Earth and Environmental Sciences, Cardiff University, Cardiff, Wales CF10 3AT, UK

interpretation for the Flatreef on the farms Turfspruit and Macalacaskop by Grobler et al. (2019) strengthens its correlation to the Critical Zone as found elsewhere in the Bushveld Complex, but suggests that the Flatreef is controlled by a distinctive structural style, the origin of which is not yet determined.

Ore-forming processes in magmatic orebodies are affected by their structural evolution (e.g. Clarke et al. 2000, 2005; Saumur and Cruden 2017; Maier et al. 2021), which also affects post-intrusion deformation of ore bodies. Studies mentioning the structure of the Northern Limb have been made at the scale of open pit outcrops (e.g. McDonald et al. 2005; Holwell and Jordaan 2006; McDonald and Holwell 2011), at kilometre scales (e.g. Nell 1985; du Plessis and Walraven 1990; Friese and Chunnnett 2004; Nex 2005; Friese 2012) and

at the scale of the whole Bushveld Complex (e.g. Clarke et al. 2009; Basson 2019), but there remain important questions about how structures may affect mineralization at the scale of 100s of m to km, which is a vital scale for extracting resources.

The aim of this study is to propose the evolution of the structure and mineralization of the Flatreef in the Northern Limb on the Turfspruit Farm study area (Figs. 1 and 2) at the deposit scale. An exploration database consisting of more than 720 km of drill core with intercepts from the Main Zone, Critical Zone and Lower Zone, detailed surface mapping, detailed geophysical surveys, and underground observations from shaft sinking for the Platreef Mine (Ivanplats (Pty) Ltd), are used to determine the evolution of the major structures that controlled the formation of the Flatreef in the study area.

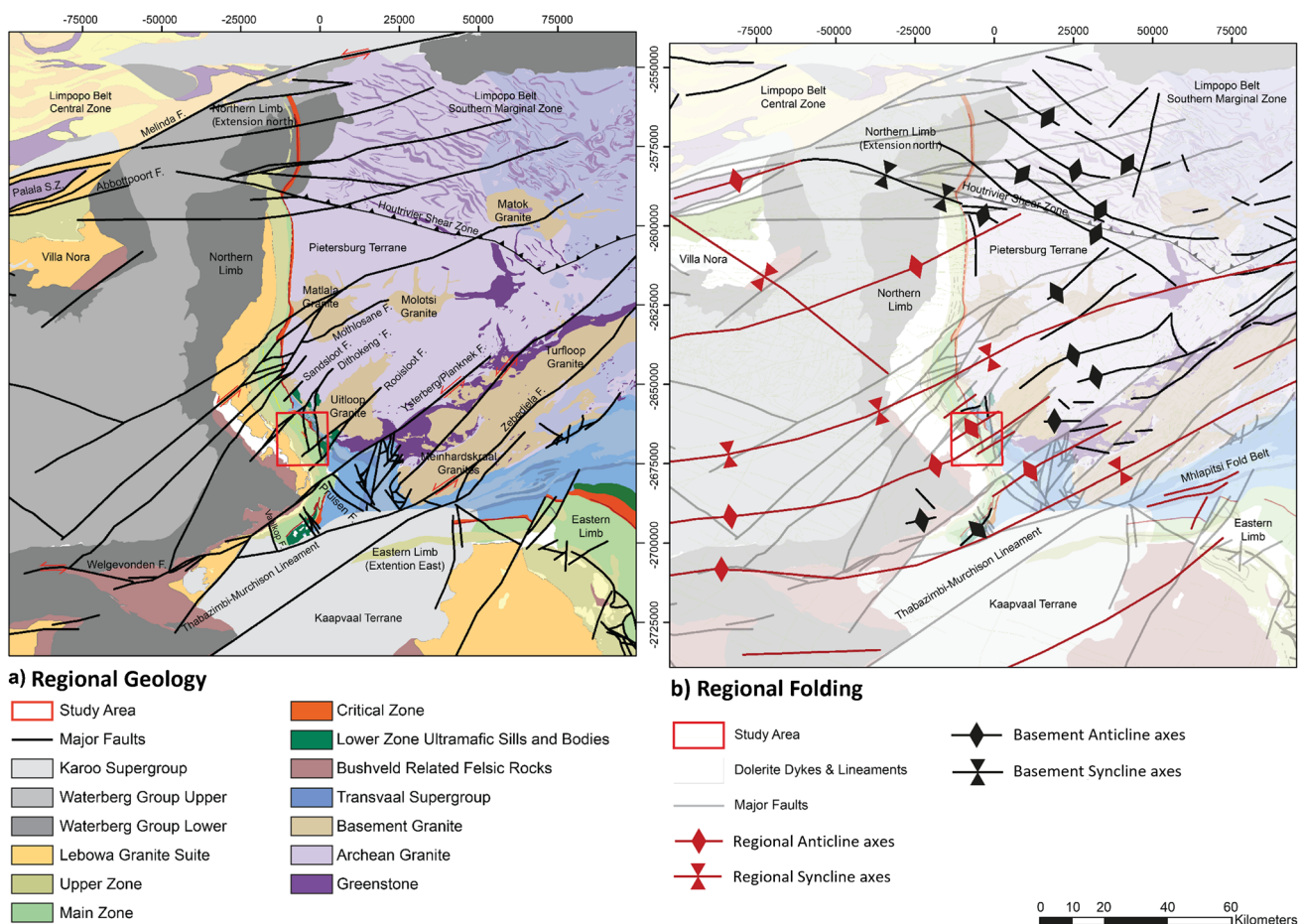
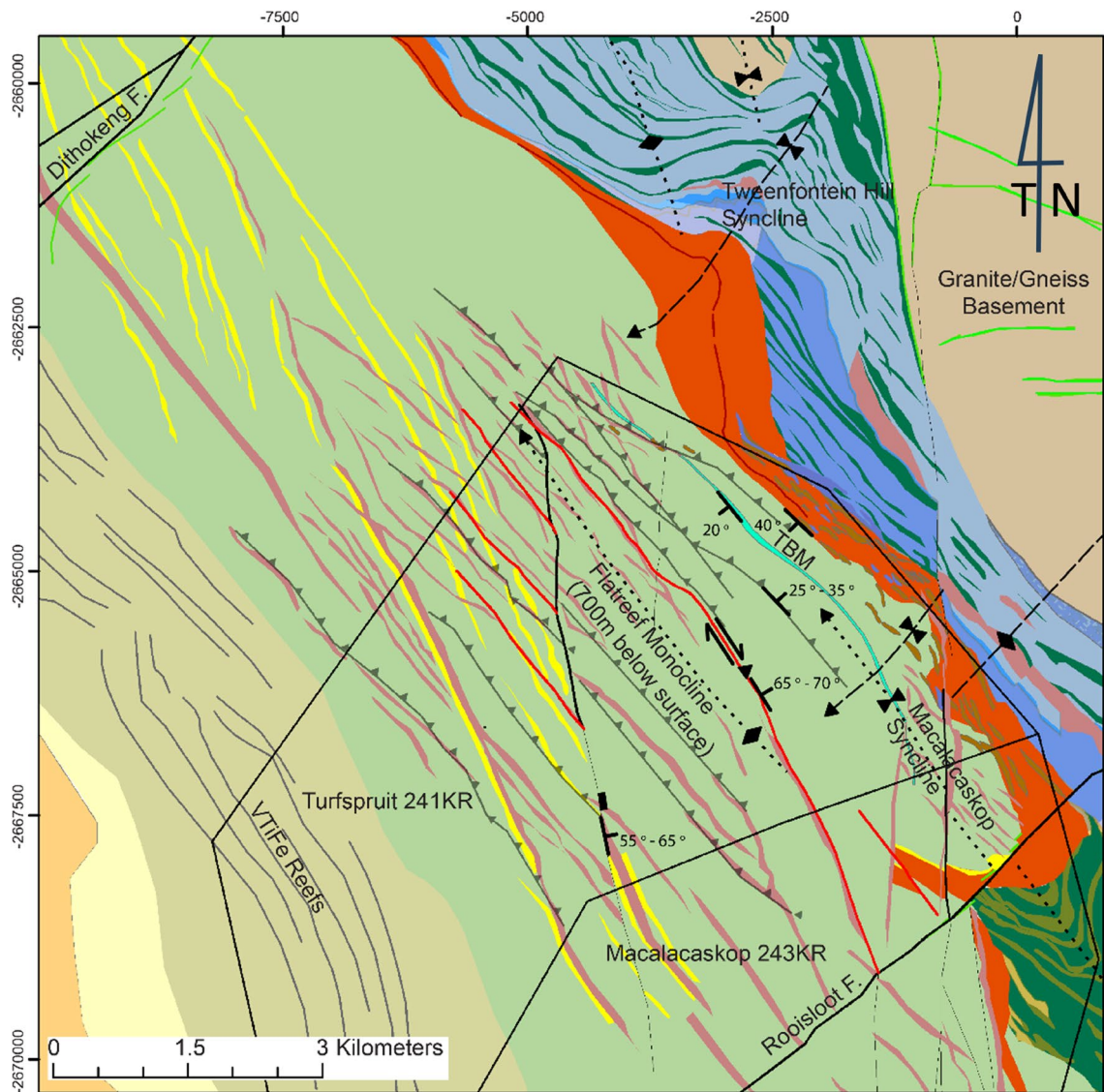


Fig. 1 (a) The regional geology and structure of the northern part of the Kaapvaal Craton. (b) The principal fold orientations. Compiled from the Council for Geosciences 1:250 000 scale regional mapping, Basson (2019), Bumbay and van der Merwe (2004), Friese

(2003) and Grobler et al. (2019). NE-SW trending open folds in the basement affect the cover rocks indicating reactivation or prolonged ductile activity



Surface Geology and Structure of Turfspruit and Surrounds

- | | |
|---------------------------------|---|
| Ivanplats Project | Upper Zone |
| Dolerite Dykes & Lineaments | Main Zone (shown with the TBM - Tennis Ball Marker) |
| Granitic Vein | Critical Zone |
| Tshukudu and subsidiary faults | Lower Zone Ultra Mafic Sills and Bodies |
| Nkwe and subsidiary faults | BIC Felsic Rocks |
| Low-angle faults – near surface | Upper Pretoria Gp Metamorphosed Sediments |
| F2 Fold Axes | Timeball Hill Fm. (Quartzite, Shale) |
| F1 Fold Axes | Duitschland Fm. (Intercalated Shale, Quartzite, Dolomite) |
| Regional block faults | Penge Fm. (BIF) |
| VTiFe Reefs | Malmani Fm. (Dolomite) |
| Inferred & Mapped Anorthosite | Black Reef Fm. |
| Lebowa Granite Suite | |

Fig. 2 Near-surface geological and structural map showing the major structural features from recent detailed surface mapping and high-definition geophysical survey data. Folds at depth have been traced to surface (e.g. the Macalacaskop syncline). Section A - A' shown in Fig. 6

Regional tectonic setting

The Northern Limb occurs within the Pietersburg terrane of the Kaapvaal Craton (de Wit et al. 1992). Its eastern outcrop has a sinuous surface expression (Fig. 1), with a generally moderate westerly dip and a north–south extent of 120 km. Its floor rocks consist of the sedimentary succession of the Transvaal Supergroup in the south; to the north the intrusion cuts down into basement granite and gneiss (Kinnaird and McDonald 2005; Kinnaird et al. 2005). Hanging wall rocks consist of A-type granites of the Bushveld Complex, and clastic sedimentary rocks of the Waterberg Group (Fig. 1a).

The northern limit of the surface expression of the Northern Limb is defined by the Melinda Fault (Fig. 1) that extends east along strike of the Palala Shear Zone (PSZ). These two structures are also referred to by a variety of other names such as the Palala-Zoetfontien Lineament (Schaller et al. 1999). These structures form the regional boundary between the Central and Southern Marginal Zones of the Limpopo Belt (Brandl and Reinold 1990; Schaller et al. 1999; Bumby and Van der Merwe 2004). The northern extremity of the Northern Limb (traced north-westwards to the Villa Nora Segment: van der Merwe 1976), has recently been extended 25 km due north below Waterberg Group metasedimentary rocks (Kinnaird et al. 2017).

The Thabazimbi–Murchison Lineament (TML) separates the Northern Limb along its southern boundary from the main Bushveld Complex (Fig. 1a). The TML defines the boundary between the Pietersburg terrane and the central part of the Kaapvaal Craton and was formed due to continental-scale, SE-directed transpression between the Zimbabwe and Kaapvaal cratons in the Archean (Good and De Wit 1997). The TML may have played a critical role in the intrusion of the Bushveld Complex (Du Plessis and Walraven 1990; Kinnaird et al. 2005), although McDonald and Howell (2011) have argued that while the complex may have intruded along the axis of the TML, the lineament was a barrier between the Northern Limb and the rest of the Bushveld.

Regional folds are dominated by NE–SW upright F_1 open folds (Fig. 1b). Although these folds affect all Northern Limb rocks and the overlying Waterberg Group, they may have been initiated before Northern Limb intrusion (Du Plessis and Walraven 1990). Tweefontein Hill, situated NNE of the study area, exposes a southwest plunging F_1 syncline within the floor rocks to the Northern Limb (Nex 2005) (Fig. 2). F_1 folds have been refolded during a later subordinate deformation event (D_2) of ENE–WSW shortening that formed fold axes striking NNW–SSE to N–S (Nex 2005). Friese (2012) recognised that this D_2 deformation event influenced rocks of the Northern Limb and not just the floor rocks at Tweefontein Hill.

Two principal fault orientations dominate within the Pietersburg terrane (Meinster 1974; Van der Merwe 1978; Du Plessis 1987; Du Plessis and Walraven 1990). These are NE–SW to ENE–WSW-orientated faults, of which the Ysterberg–Planknek (YPF) and Zebediela Faults are the most prominent (Fig. 1a), and N–S to NNW–SSE-orientated faults which are dominant in the southern part of the Northern Limb. The latter faults are characterised by red to pink granite intrusions.

The YPF is a post Transvaal Supergroup re-activated deformation zone (De Wit et al. 1992; Good and De Wit 1997), with a sinistral separation of up to 6 km (Geological Survey of South Africa 1978). Numerous NE–SW faults (such as the Rooisloot, Dithokeng, Sandsloot and Mothlosane Faults) cut through the Transvaal Supergroup, Rustenberg Layered Suite (RLS) and younger roof rocks north of the YPF (Fig. 1a). The NE–SW faults are interpreted as growth faults during emplacement of the Northern Limb causing on-lapping or transgressional relationships of the Northern Limb stratigraphy along strike (Van der Merwe 1978).

The map scale separations on NE–SW trending faults in the Northern Limb are predominantly sinistral (Fig. 1a). A sinistral shear sense has been noted on the sub-parallel PSZ by McCourt and Vearncombe (1987, 1992) and Brandl and Reimold (1990). However, the PSZ has a dextral strike slip net displacement, which was the result of NNW–SSE shortening and transpression (Holzer et al. 1998; Schaller et al. 1999) between 2053.5 ± 9.9 Ma and 1971 ± 26 Ma (Liang et al. 2021). The most likely age for this deformation is c. 2025 Ma (Liang et al. 2021). This dextral displacement may therefore postdate syn-Bushveld sinistral movement.

Basson (2019) noted that the F_1 fold orientations are parallel to the NE–SW faults. F_1 folds may have been amplified along the southern boundary of the Northern Limb, near the TML. This is consistent with the gradual decrease in fold amplitude to the north in the Northern Limb, as noted within Angloplats' Mogalakwena Mine on Sandsloot Farm 236 KR, described in detail by Friese (2012), Nex (2005) and Armitage (2011).

Overview of the study area

The study area is in a fault block delimited by the NE- to ENE-trending Dithokeng and Rooisloot Faults to the north and south of the block respectively (Fig. 2). In the study area the RLS attains a thickness of approximately 7500 m (Grobler et al. 2019). The lower stratigraphic units of the RLS include the Lower Zone at its base (outcropping east of the study area), overlain by the Lower and Upper Critical Zone correlatives as described by Grobler et al. (2019) (Fig. 2). These units are situated below the Main Zone and

correlate with the Critical Zone lithologies of the RLS as found elsewhere in the Bushveld Complex and along the Northern Limb. To the west of the study area the Main Zone is overlain by the Upper Zone. The Lower and Upper Critical Zones together reach a thickness of up to 600 m in the Flatreef, inclusive of xenoliths, 700 m below surface. Their thickness near surface is highly variable, but is generally less than 400 m, and they have a dip of 35° WSW at surface (Fig. 2).

The Lower and the Critical Zones intruded into shallow marine to continental shelf clastic sedimentary rocks of the Deutschland Formation at the base of the Pretoria Group (Eriksson and Reczko 1995) and the underlying Penge and Malmani Formations, and the Blackreef Formation in places (Fig. 2). The Deutschland Formation attains a maximum thickness of 1000 m to 1200 m in the study area (Warke and Schroeder 2018). Sedimentary xenoliths of the Deutschland Formation (shale and dolomite/limestone) and overlying Timeball Hill Formation (shale and quartzite) are found within the lower stratigraphic units of the magmatic sequence, mainly within the Lower Zone and Critical Zone (Grobler et al. 2019). The floor contact of the RLS to the east of the study area is not well defined but appears to occur near the unconformity of the basement granite and gneiss with the platform carbonates of the Malmani Subgroup (Chuniespoort Group).

Lower Zone rocks are found as sill-like intrusions within the sedimentary rocks and as layered bodies, exposed at surface, along strike and close to the lower contact of the sedimentary rocks with the basement (Van der Merwe 1976) (Fig. 2). Where the Lower Zone intruded near the contact with the basement rocks, Lower Zone bodies are developed mostly along the downthrown (southern) side of the regional scale NE–SW faults (Fig. 1a), showing that these faults accommodated and controlled intrusion.

The Flatreef, which includes the gently dipping mineralized correlatives of the Merensky and Bastard Cyclic Units (Grobler et al. 2019), occurs between 600 m and 800 m below surface, extending down dip and westwards to 1100 m. Upper Critical Zone layering undulates due to folds (Figs. 3, 4 and 5). The amplitude of the undulations in the magmatic layering diminishes upwards within the Main Zone, so that the anorthosite layers of the upper Main Zone and Upper Zone conform to the general NNW–SSE strike and WSW dip of the RLS in the area (Fig. 2). The anorthosite layers define robust linear trends (negative anomalies) which are observed in the detailed aeromagnetic survey (Fig. 3). These layers have a constant strike of 334° over more than 6 km (Fig. 3). The regularity of the Upper Zone anorthosite layers is in striking contrast to observations of the anorthosite layers within the norite cycles of the Merensky and Bastard Cyclic Units of the Flatreef in underground excavations. As the undulations in the magmatic

layers decrease upwards, so the general dip of the layering becomes approximately constant, for example, the Tennis Ball Marker unit dips about 20° WSW (Fig. 6).

In chronological order of formation the major groups of structures in the study area are F1 folds, F2 folds and thrusts, steeply dipping shear zones, and the steeply dipping Tshukudu fault. Granite dykes intrude the reverse faults and steeply dipping shear zones. All structures show evidence of a complex history with reactivation.

F1 folds

F₁ folds are found within the footwall of the Critical Zone to the east of the study area (Fig. 3). These open folds have gently south-west plunging hinges (e.g. the Tweefontein Hill syncline) (Nex 2005) which are slightly curved by the second folding event (Fig. 3).

F2 folds and reverse faults

F₂ folds have moderately to steeply east dipping axial surfaces and fold hinges that plunge gently NNW. A north-south F₂ open fold within the upper strata of the Chuniespoort Group occurs in the central part of the study area at depth (Fig. 4). This F₂ fold becomes more pronounced southwards where it outcrops on Macalacaskop farm as a north plunging anticline with adjacent syncline within quartzite of the lower units of the Pretoria Group sedimentary rocks (Figs. 2 and 4).

Layer parallel and sub-parallel reverse faults and duplexes are undulating, southwest verging structures that dip 35° to 45° towards the NE or ENE and have a vertical spacing of 100 to 150 m (Figs. 5 and 6). The reverse faults in the study area cut all litho-stratigraphic boundaries and extend from the lower units of the Flatreef into the Main Zone. The structures utilise weak zones formed by competence contrasts between different rock types within a stratigraphic unit, and by stratigraphic boundaries (cf. Friese 2012) (Figs. 5 and 6). Core intercepts show that slip-planes have variable characters and infills, indicating the influence of several deformation episodes (Fig. 7b). Fault planes are planar or reactivated surfaces with gouge up to 10 mm thick of serpentine, chlorite/talc or quartz-carbonate and calcite. Although individual fault planes and shears do not have extensive continuity along strike or dip, they form well-developed duplex structures that can be traced between drill intercepts and underground exposures (Figs. 6 and 8). Lateral and frontal ramps developed in complex duplex structures. Displacements cannot be determined from core.

Observations from underground development show that brittle extensional reactivation of the bounding thrust planes, and associated granite dykes, is characteristic of the reverse faults extending through the Main Zone. Later infill

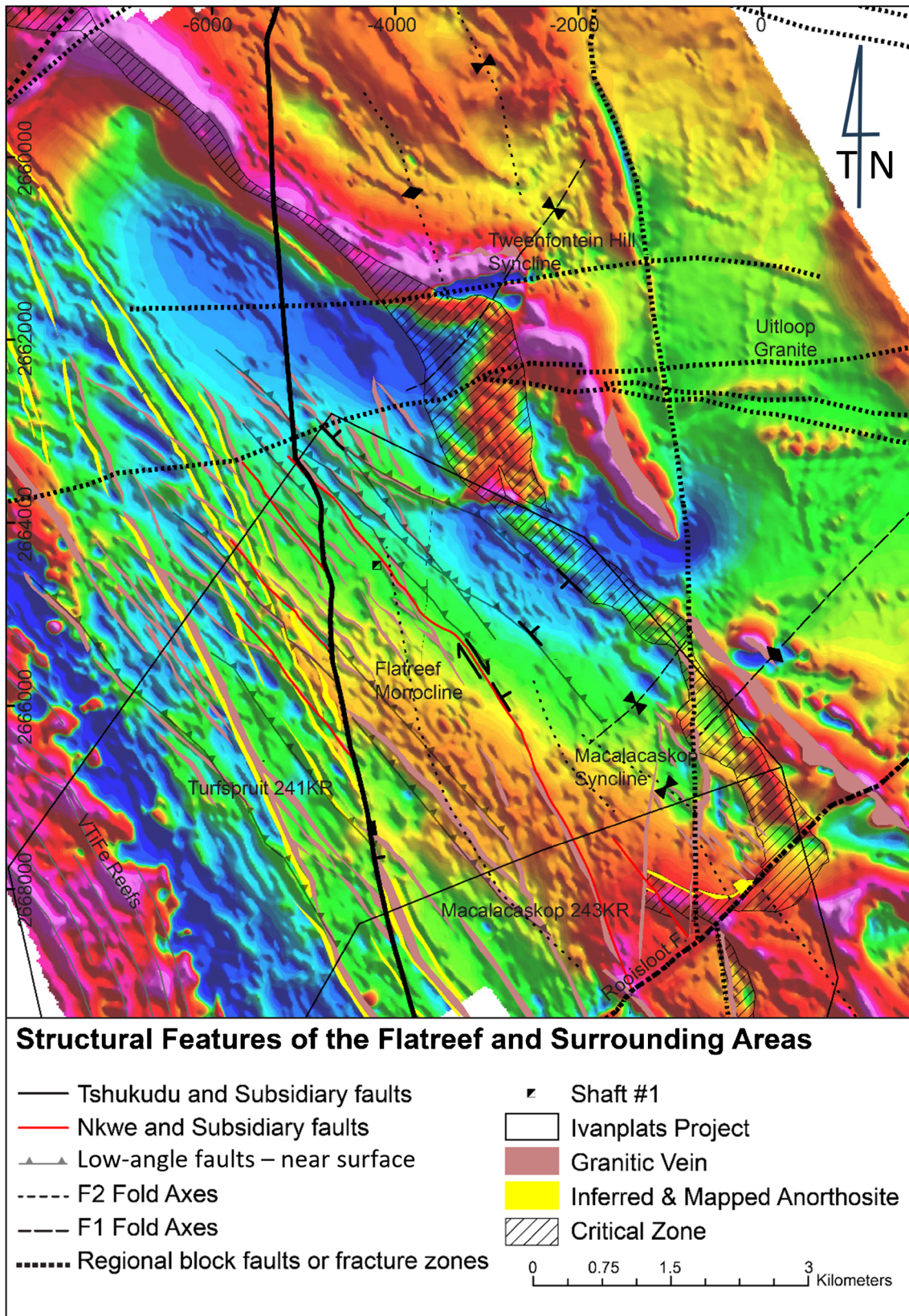
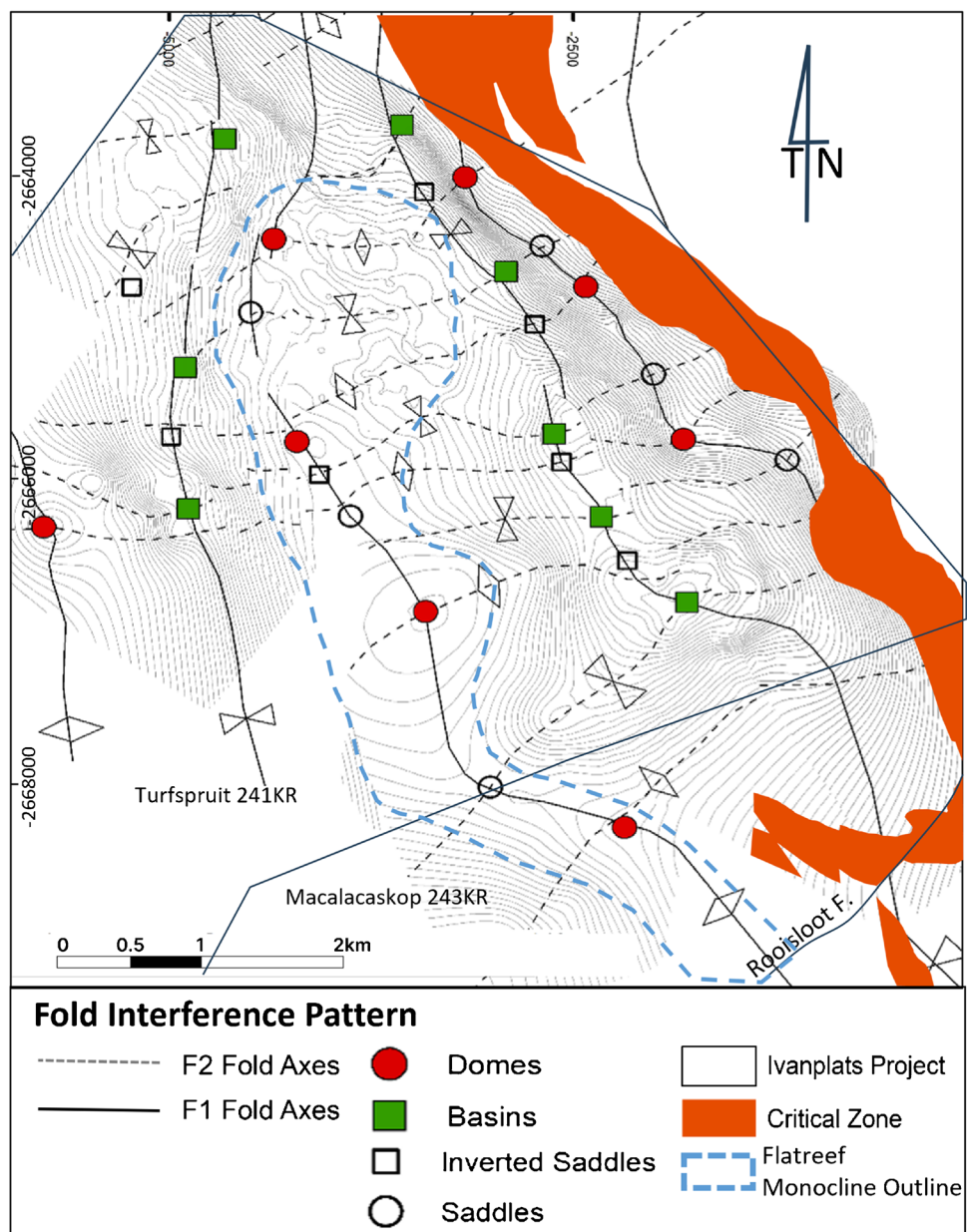


Fig. 3 A total magnetic intensity image of the Flatreef study and surrounding areas, overlaid with the structural model. Granite dykes create linear, highly magnetic anomalies and the anorthosite layers are low-magnetic anomalies at slightly oblique strike angles to the granite dykes

Fig. 4 Plan view of major NE-trending F_1 and subordinate NW-trending F_2 fold axes on an interpolant surface created from the upper contact of the Footwall Assimilation Zone (FAZ) (after Grobler et al. 2019), with an approximation of the Flatreef Monocline extents outlined



can include quartz-feldspathic, quartz-carbonate or granitic rocks. An excellent example is a fault intersected 450 m below surface within Shaft #1 that shows brittle extensional overprinting of the fault and the associated granite dyke (Fig. 7a). The granite dyke follows the general NE to ENE dip direction of the duplex structures, with undulating contacts indicating control on intrusion by the original fault plane geometry. Variations in dyke thickness are consistent with down-dip (NE to ENE) extensional movement of the hangingwall block along the undulating fault plane causing dilation during intrusion. Granite dykes have mylonite along their contacts and are fractured across their whole width. Alteration is evident as reddish discolouration within the intrusion, most intense along joint planes and contacts.

A notable increase in intensity of reverse faulting occurs within the cyclical units of the Flatreef stratigraphy where thrusting occurred along lithological contacts and zones of competence contrast between relatively thin layered rock types (Figs. 8 and 9). Lithological control on duplex width was noted within the underground exposures: duplexes are wider in well-layered stratigraphic units, such as the norite cycles, and where bedded sedimentary rock xenoliths occur.

The Bastard Cyclic Unit, as described by Grobler et al. (2019), was exposed for the first time during shaft sinking at 770 m depth. The cyclic norite unit is overlain by an extensively developed, mottled anorthosite, resembling the Giant Mottled Anorthosite elsewhere in the Bushveld Complex (Vermaak 1976). Layer sub-parallel deformation

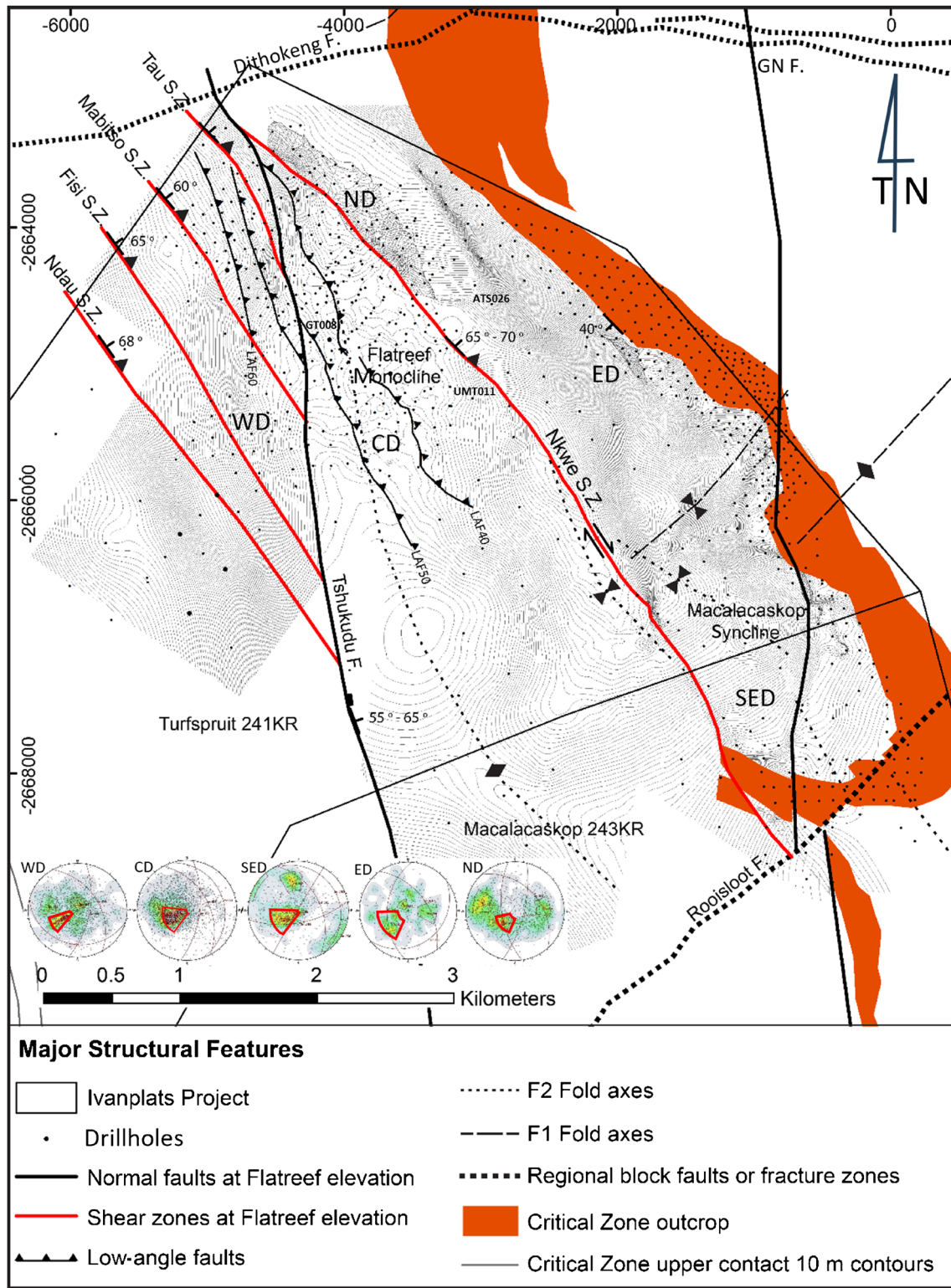


Fig. 5 Low- and medium-confidence structures (named) defining seven fault blocks across the resource area for the project on Turfspruit farm. Northwest trending steep structures are shear zones with reverse, oblique strike-slip sense of movement (shown in red). Low angle faults are shown at Flatreef upper contact intersection, approximately 750 m below surface. The base of the Main Zone (Critical

Zone upper contact) is shown as contours at 10-m-elevation intervals. Equal area, lower hemisphere stereoplots for the five structural domains (Peters et al. 2017) are shown with joint sets. Central domain (CD) has three joint sets corroborating the major orientations of the TSK, NKW and low angle faults, as discussed

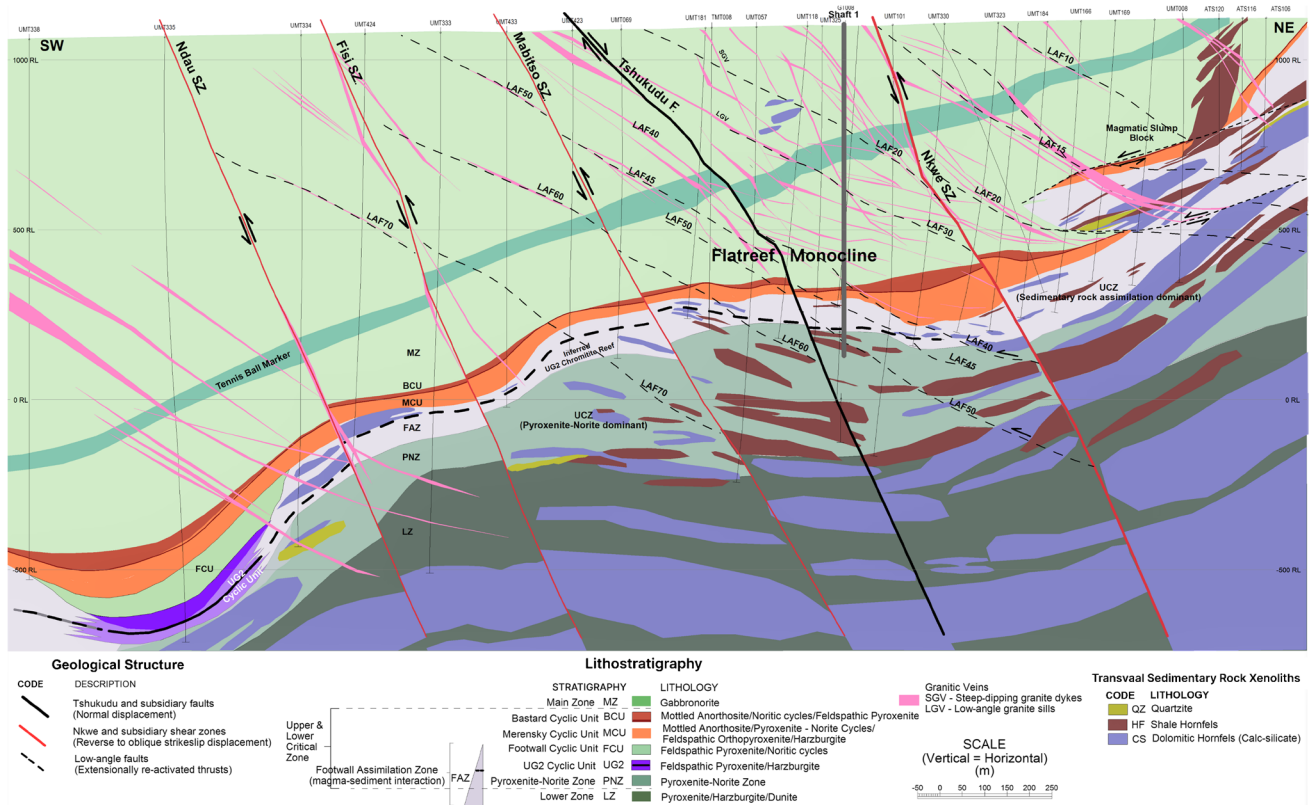


Fig. 6 SW-NE orientated vertical dip section A - A' (looking NW) of the Flatreef deposit within the shaft development area (4000 m dip extent shown, no vertical scale exaggeration). Low angle and steep

granite veins (LGV and SGV respectively) and their relation to the NE/ENE dipping thrust duplex structures are shown (after Grobler et al. 2019)

has occurred in the underlying anorthosite layers of the norite cycles forming small-scale folds, schlieren and, in extreme cases, boudinage (Maier et al. 2013). Syn-magmatic shearing ('hot' shearing: Carr et al. 1994) caused the semi-consolidated anorthositic magma to accumulate within dilation zones, locally forming Riedel-type anorthosite apophyses between thrust planes (Fig. 8). The primary shear planes may not be well preserved, as, for example, within the immediate hanging wall to the Bastard Cyclic Unit (Fig. 8 Insert 1).

Another example of syn-magmatic ductile deformation occurs within the hanging wall of a thrust zone exposed within the shaft at 450 m depth within a layered melagabbro-norite-anorthosite unit of the Main Zone. A steeply east dipping, extensional fault plane is preserved below a small pothole structure (Fig. 10). Localised extension formed the mini-pothole by extension between boudins due to magma slumping. The mini-pothole was infilled by anorthositic magma. The adjacent layers form scar folds where they have been displaced into the gap created by the mini-pothole.

Lower in the shaft at 780 m depth, the base of the norite cycles is in contact with the underlying Bastard

Reef pyroxenite. Here the fault structure exhibits magmatic shearing with a brittle extensional overprint (Fig. 9). The sole of the duplex structure obliquely cuts the lower contact of the cyclical norite unit with the Bastard Reef pyroxenite (Grobler et al. 2019). The upper contact of the Bastard Reef pyroxenite (which forms the basal layer of the Bastard Cyclic Unit) shows layer-parallel to sub-parallel fault planes with lateral and frontal ramps over a width of 50 cm (Fig. 9). The fault zone undulates with foliation developed in the pyroxenite host rock and tension fractures splaying into the hanging wall and footwall (Fig. 9). In contrast, the overlying anorthosite is deformed by sub-parallel to obliquely cross-cutting thrust planes within the magmatic layering, which causes an undulating, diffuse upper contact with the overlying norite cycles. Low-temperature alteration assemblages are focussed along the lower bounding fault plane. Reactivation has formed a fault gouge that was infilled and partially healed by calcite-rich material (Fig. 9).

Measurable kinematic indicators are limited to striations that formed along fault planes where chlorite/talc assemblages occur as infill, mostly preserved within the pyroxenite units. Slickensides show multiple displacement directions;

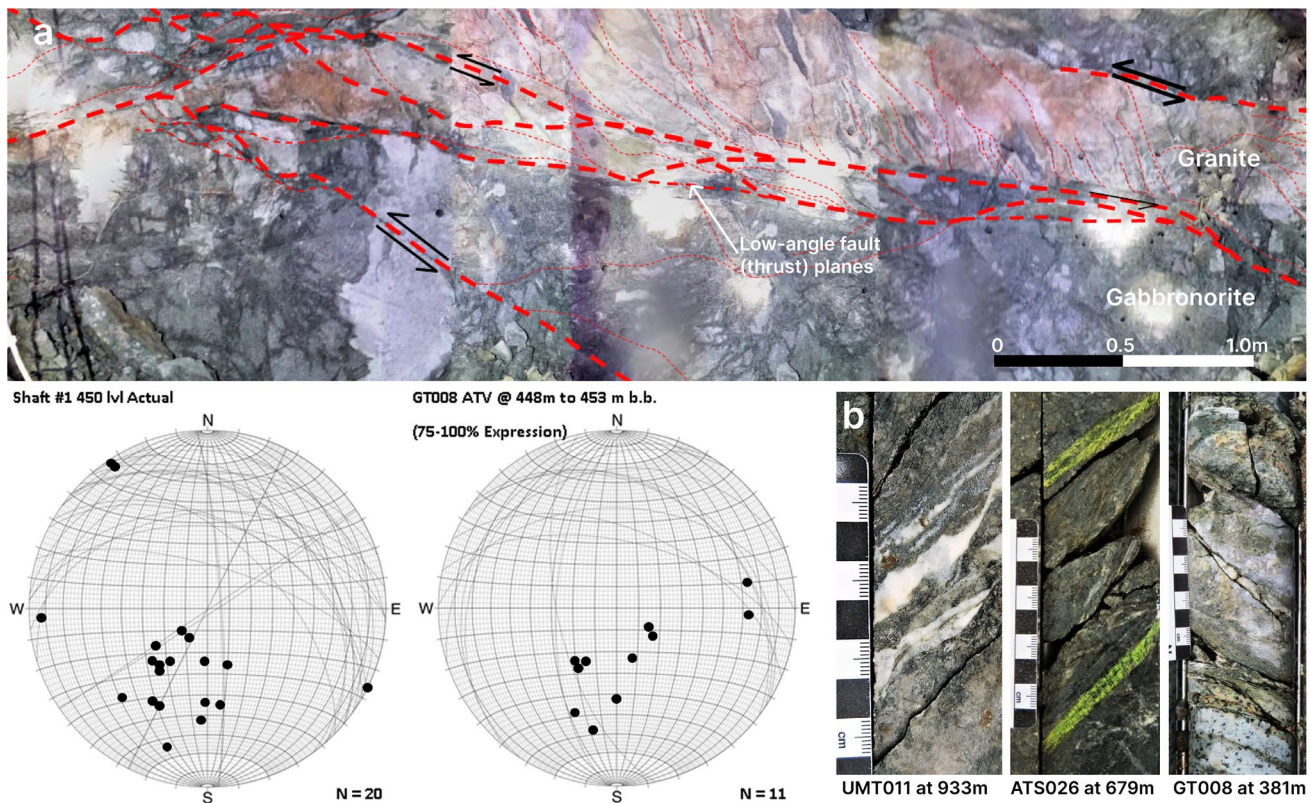


Fig. 7 Features of a thrust duplex mapped at the 450 level station in Shaft 1 (445 m below surface). Equal area, lower-hemisphere stereoplots confirm the ENE to NE dip direction of the structure. The stereoplots show a good correlation between planar structural features of the acoustic tele-viewer data (from the shaft geotechnical borehole) and the shaft mapping. Core photographs of UMT110, GT008 and ATS026 ((b)), with drillhole positions shown in Fig. 5) show exam-

ples of thrust faults in drill core. A granite dyke shown in the photo mosaic (a) of the shaft's north-eastern wall, was intruded along the thrust fault of the thrust duplex structure. The dyke shows local thickening and mylonite development along its contacts. Internal fractures within the granite (not indicated) show post-intrusion deformation of the granite magma

oblique slip of the hangingwall towards the SW is most prominent.

Steep shear zones

Six shear zones dipping 60° to 70° ENE have been mapped in the study area (Figs. 5 and 6). The undulating shear zones comprise multiple anastomosing shear planes and show oblique reverse to right-lateral strike-slip movement with vertical components from ca. 5 m to 30 m. The shear zones are mylonitic, modified to cataclasites where extensional reactivation occurred. Cataclastic quartz-carbonate infill is generally less than 2 m thick with healed fracture zones up to 5 m wide into hanging wall and footwall blocks. Partial healing by red to pink granophyric or quartzo-feldspathic rock is characteristic, like the N–S faults described by Van der Merwe (1976).

The most prominent shear zone, the Nkwe Shear Zone, creates a strong linear anomaly in the surface weathering profile (Peters et al. 2017). The Nkwe Shear Zone forms the

eastern boundary of the Flatreef, parallel to the eastern axis of the monocline in the upper contact of the Flatreef (Fig. 4). Although there appears to be no clear expression of the feature within the gravity or magnetic data, the Nkwe Shear Zone is defined by 124 drill core intersections along a strike length of 5000 m to a depth of 1200 m below surface. The thickness of the shear zone varies from 0.15 m to 10.1 m, with an average of 1.3 m. The shear zone generally dips 67° ENE to NE (Fig. 6), and undulates in strike and dip. A zone of foliation development and fracturing of the host rock extends up to 10 m into the hanging wall or footwall of the structure. Scarce movement indicators indicate reverse dip-slip movement with a vertical displacement of up to 30 m. Reverse offset has been confirmed from displacements of marker layers in the Main Zone noted in drill core such as the Tennis Ball Marker Unit, approximately 200 m above the base of the Main Zone (Figs. 2, 6 and 11),

More detail on the Nkwe Shear Zone can be seen within a box cut excavation for Shaft #2 of the Mine development. The excavation exposed the structure along its

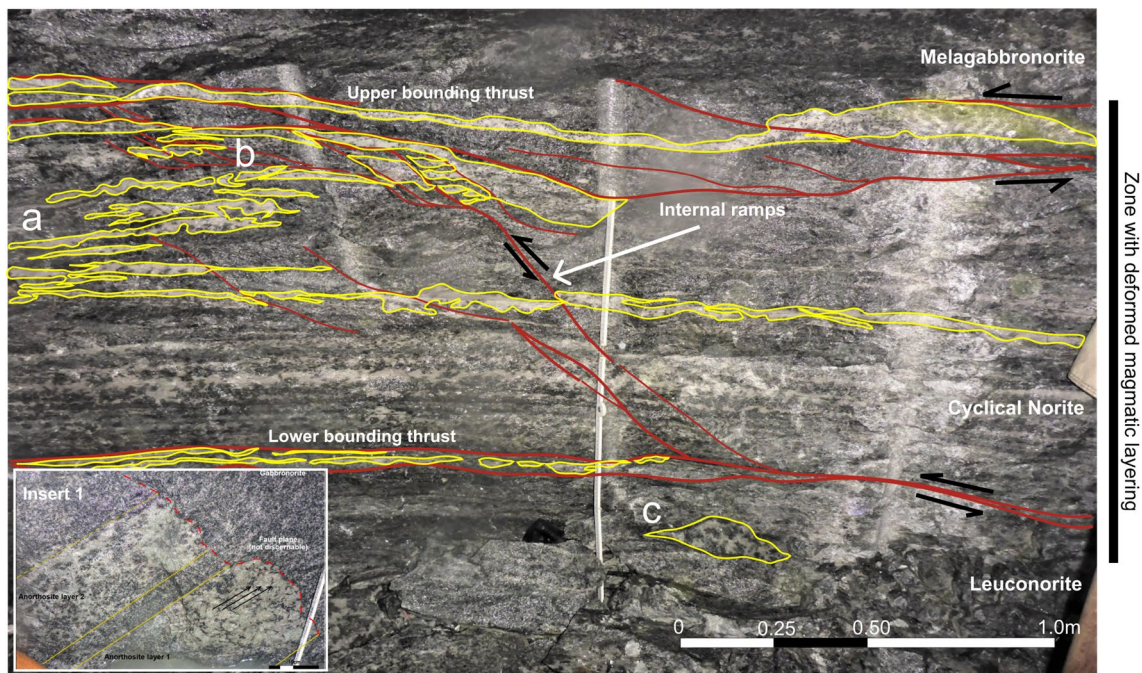


Fig. 8 Syn-magmatic deformation in the NE sidewall of Shaft #1 in the upper part of the norite cycles for the Bastard Cyclic Unit at 775 m below surface. Anorthositic layers and boudins are outlined in yellow. The main tectonic features are shown in red. (a) Anorthositic magma formed schlieren and lenses in association with dilational zones created within the footwall to an internal ramp feature; (b) Small scale drag folds developed within anorthosite layers; (c) Anorthositic boudins formed within a layer-parallel extensional struc-

ture. Gradational decrease in magma response to the thrust fault can be seen into the footwall block. Insert 1: Shaft #1 north-eastern sidewall at 773 m below surface showing the offset of an anorthosite layer by a ramp plane (part of a thrust duplex shown in Fig. 8). The ductile character of this hot shear is evident in the striations and boudins formed by the feldspar and pyroxene, respectively. Striations indicate oblique right-lateral strike-slip displacement

north-western and eastern sidewalls to a depth of 29 m below surface and along a strike length of 60 m. The Nkwe Shear Zone consists of partially healed fault rocks and intrusions up to 5 m wide. A large portion of the shear zone has been intruded by a granite dyke (Fig. 12). The dyke has undulating contacts with intense fracturing and brecciation. Most of the dyke is intensely jointed with numerous small-scale mylonitic, Riedel and vein-parallel shears. Mylonites may occur at the edge of the dyke. The remainder of the shear zone consists of intensely fractured and sheared Main Zone gabbronrite. Both the hanging wall and footwall contacts have been overprinted by reactivation, showing multiple fault planes with Riedel shears containing carbonate infill. Part of the eastern sidewall has intense jointing in the hanging wall block of a reverse fault close to the top of the Nkwe Shear Zone.

Along the western sidewall exposure of the Nkwe Shear Zone, north-easterly dipping reverse faults (pre-dating the shear zone) are terminated against it. Reverse separation of approximately 2 m can be determined from the vertical offset of the reverse faults. This separation at 29 m below surface is much less than the 60 m separation where the Nkwe Shear Zone intersects the Flatreef structure 700 m below surface.

Alteration is dominated by chloritization of host rock with occasional sericite/albite and potassic alteration. Alteration selvages vary between 2 and 10 m in width. Sulfide mineralisation due to hydrothermal remobilisation in association with quartz-feldspar gouge in-fill is common within the cataclasite.

Granite dykes

Granite dykes observed in underground development and drill core could also be detected in the aeromagnetic survey, in which they have distinct positive linear magnetic signatures. The dykes crosscut the magmatic layering (Fig. 3). The dykes intruded into the NNW–SSE striking shear zones, thus partially healing and mostly obscuring the original mylonites. Granite dykes are dominant within the Main Zone but pinch out downwards towards the Critical Zone (Fig. 6). The dykes are a distinct pink-red colour. Granite dykes with strikes varying between NW–SE and NNW–SSE and dips less than 45° intruded into reverse-fault duplexes. These dykes have shorter strike extents than the steep dykes. They traverse the Critical and Main Zones and are more pronounced within the Critical Zone (Fig. 6)

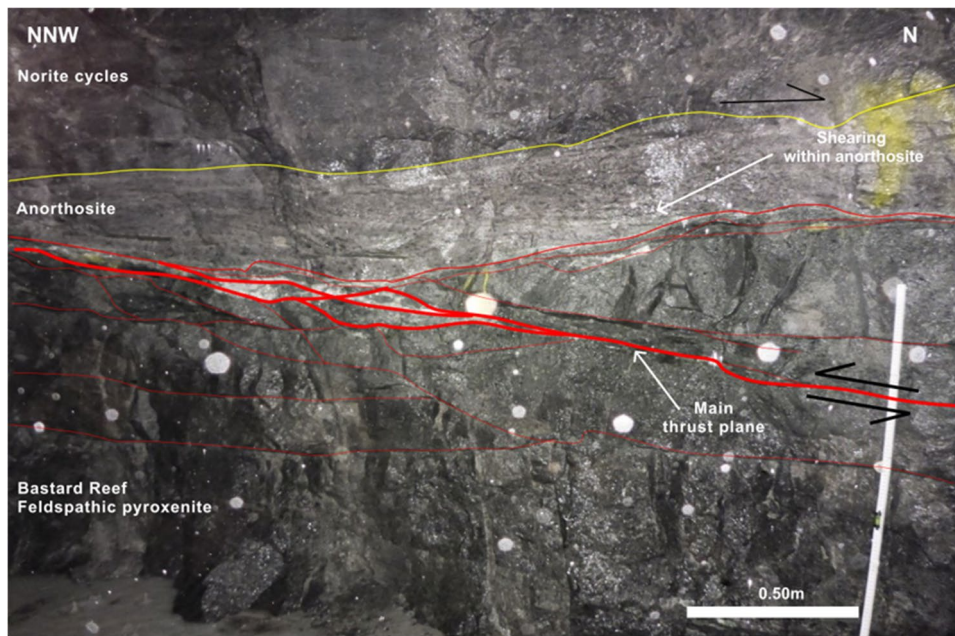
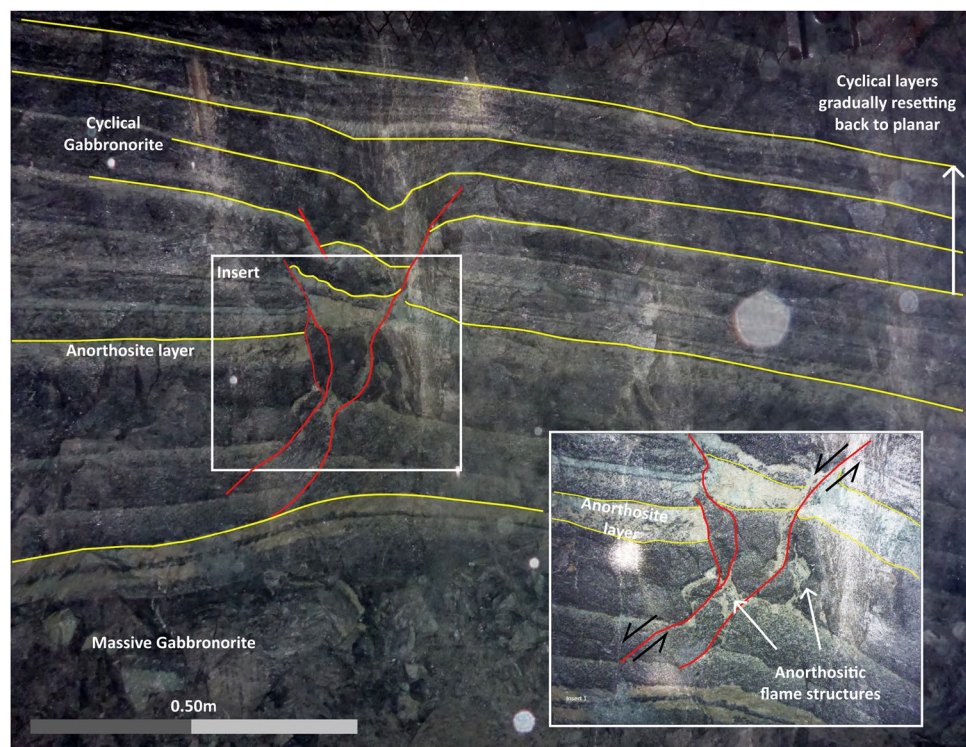


Fig. 9 The upper contact of the Bastard Reef, part of the Bastard Cyclic Unit (after Grobler et al. 2019) at 780.1 m below surface in Shaft #1. The photo shows evidence of a reverse fault duplex with steeper ramp planes developed (all fault planes are shown in red). White infill along the main shear plane is fine-grained feldspar-rich material. Note the thickening of the feldspathic pyroxenite, the foot-

wall to the reverse fault and the offset thickening of the hanging wall anorthosite above the principal fault plane. Weak internal layering within the anorthosite shows ductile response of the anorthositic magma to strain experienced during reverse faulting event. Later brittle extensional reactivation is evident within the footwall of the thrust

Fig. 10 Syn-magmatic deformation in Shaft #1 at 307 m depth. The photo of the eastern sidewall shows the shaft intersecting a 3-m-wide, sub-horizontal, layered unit 15 m above the Tennis Ball Marker. Disruption of the layering is caused by a steep extensional fault that caused magmatic slumping into a dilational zone formed between boudins within the hanging wall of the fault. Small-scale drag and roll-over folds developed within the layers below the slump structure. Anorthositic magma accumulated in dilational zones forming flame structures along the lower part of the slump structure



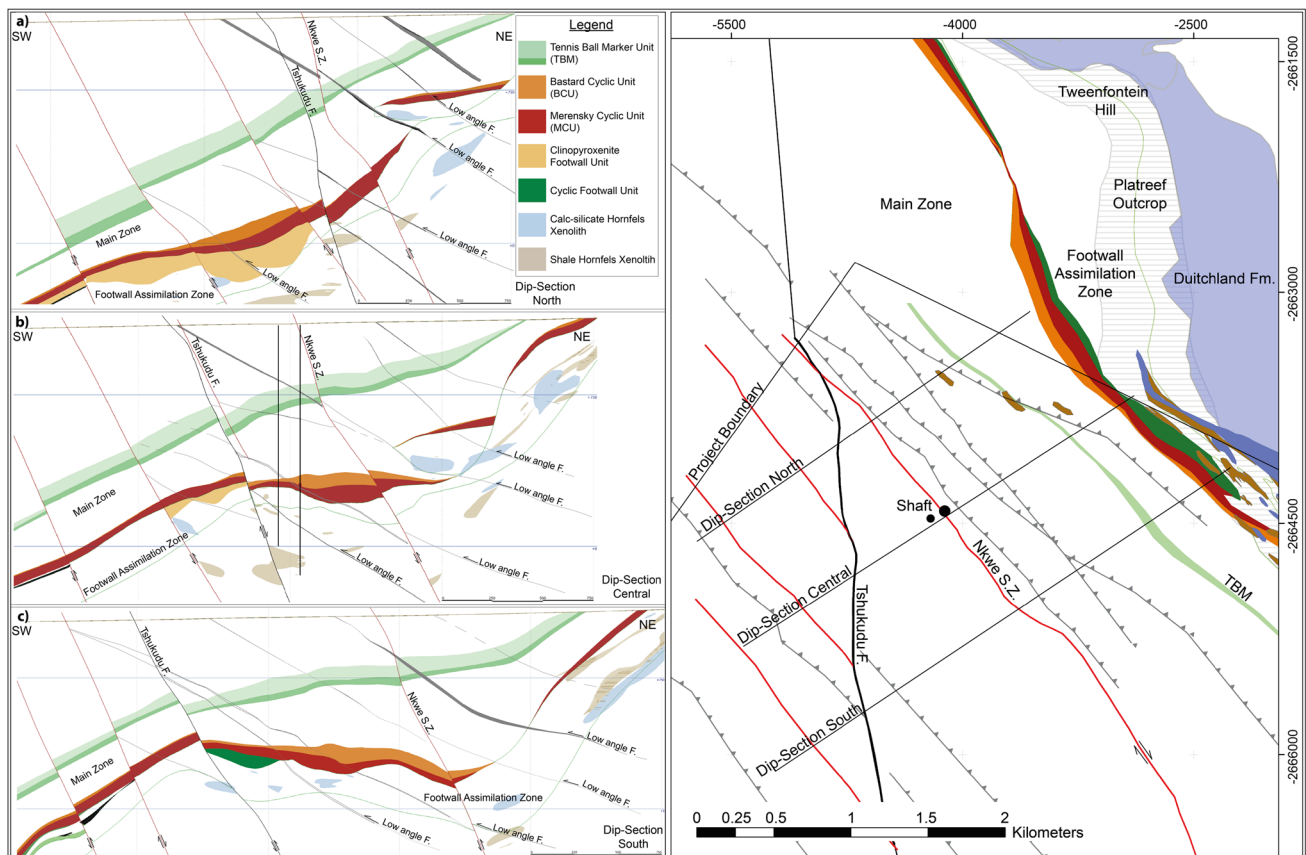


Fig. 11 SW–NE-orientated vertical dip-sections (looking NW) across the Flatreef deposit, spaced 500 m apart. The dip-sections show the control of growth faulting on the litho-stratigraphy from north-west to south-east. The Upper Critical Zone stratigraphy progressively thickened within the footwall blocks to the steep structures which acted as growth faults during Critical Zone intrusion and consolidation. The Bastard and Merensky Cyclic Units show thickening

where they are distinctly white to light grey due to sodium-rich feldspar, like the quartzo-feldspathic veins mentioned by van der Merwe (1978).

The Tshukudu Fault

The Tshukudu Fault is a major anastomosing fault zone that dips 65° east. It cuts the western part of the Flatreef, sub-parallel and close to the axial plane of the Flatreef monocline in the study area (Fig. 6). Data from 129 drill-core intercepts show the fault zone is 0.6 m to 26 m wide, with an average of 7.6 m. The Flatreef and its host magmatic units have vertical separations in a normal sense of up to 60 m across the fault zone (Fig. 6). Fault surfaces may be polished or show multiple orientated fibrous striations. Faults may have a millimetre-scale chlorite infill. Metre-scale cataclastic breccia zones and imbricate fractures may occur within the wide hanging wall fracture zone close to the main structure. The main fault gouge consists of friable carbonate and

controlled by the Nkwe Shear Zone. **a)** Development of thick, mineralised clino-pyroxenite in the footwall block. **b)** Local thickening of the Merensky Cyclic Unit within the Nkwe footwall fault block as result of reverse movement along the Nkwe shear zone. **a) to c)** The orientation of the Main Zone basal contact changes from flat, where overlying the Flatreef monocline, to easterly dipping, as the western limb of a syncline developed further south on Macalacaskop

chlorite/talc. Alteration is dominated by chloritization of the host rock, with occasional sericite/albite. Alteration selvages vary from 5 to 50 m wide, dependent on the intensity of fracturing. The Tshukudu Fault shows no expression within the magnetic survey data. It is similar to N–S faulting described by Anhaeusser and Wilson (1981) crossing the Pietersburg Greenstone Belt to the east of the Northern Limb.

Metamorphism, metasomatism and alteration

Xenoliths are found throughout the stratigraphy. There is a marked increase in xenolith occurrence within the footwall units below the Merensky Cyclic Unit of the Flatreef section (Wallmach et al. 1989; Grobler et al. 2019) and in the up-dip regions towards the east of the Flatreef and the Nkwe Shear Zone (Fig. 6). The xenoliths were originally sedimentary rocks which have been partially melted and metasomatised and are commonly crystalline. Contacts between metasedimentary and intrusive rocks are variable and can

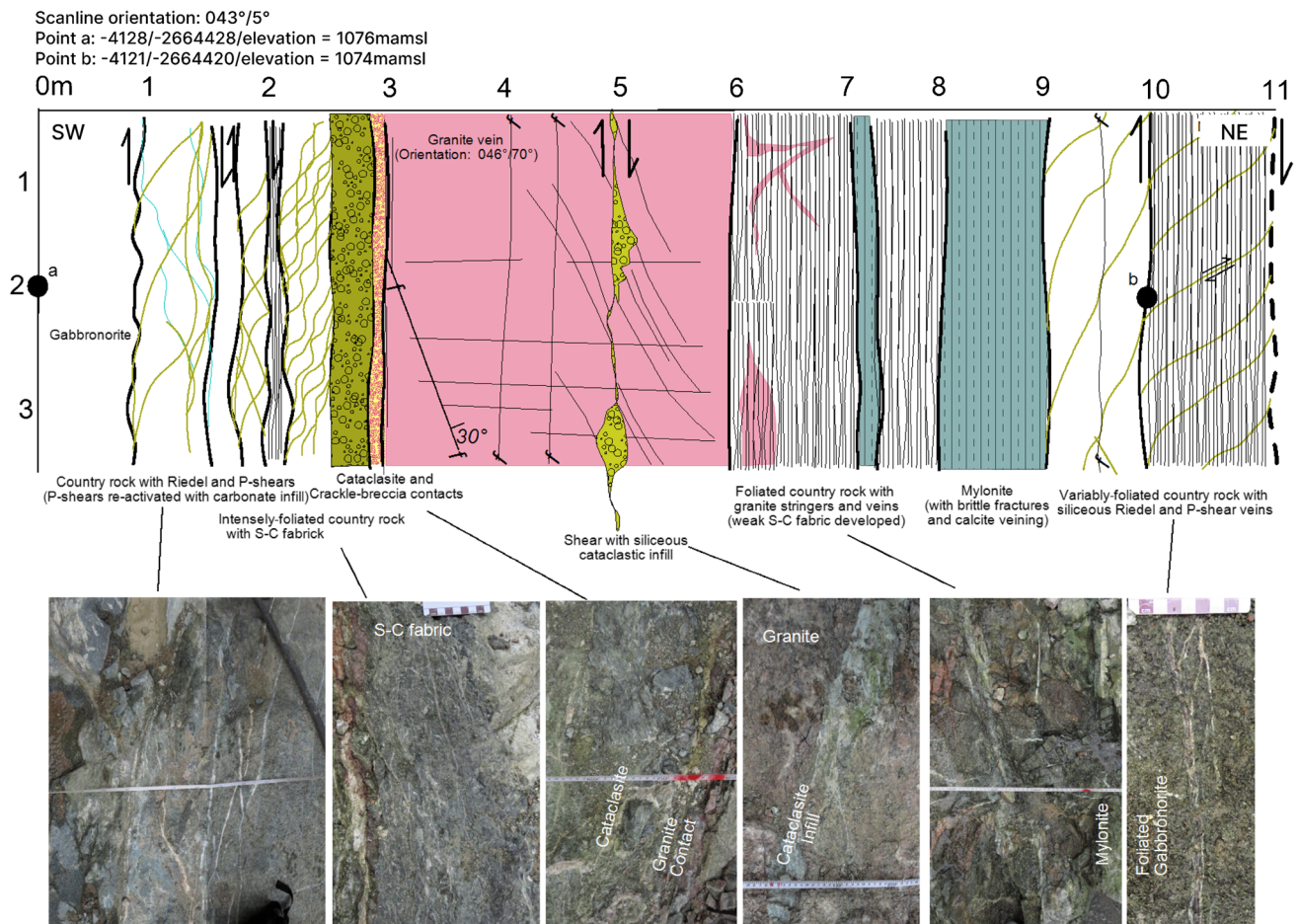


Fig. 12 A detailed map of the Shaft #2 box-cut excavation floor, 29 m below surface across a section of the Nkwe Shear Zone from the south-west (footwall block) through the shear zone and into the

hanging wall block (north-east side). The fault has been intruded by a 3 m wide granite dyke. Foliation, S-C fabric, Riedel shears, cataclastic overprinting and remnant mylonite are visible

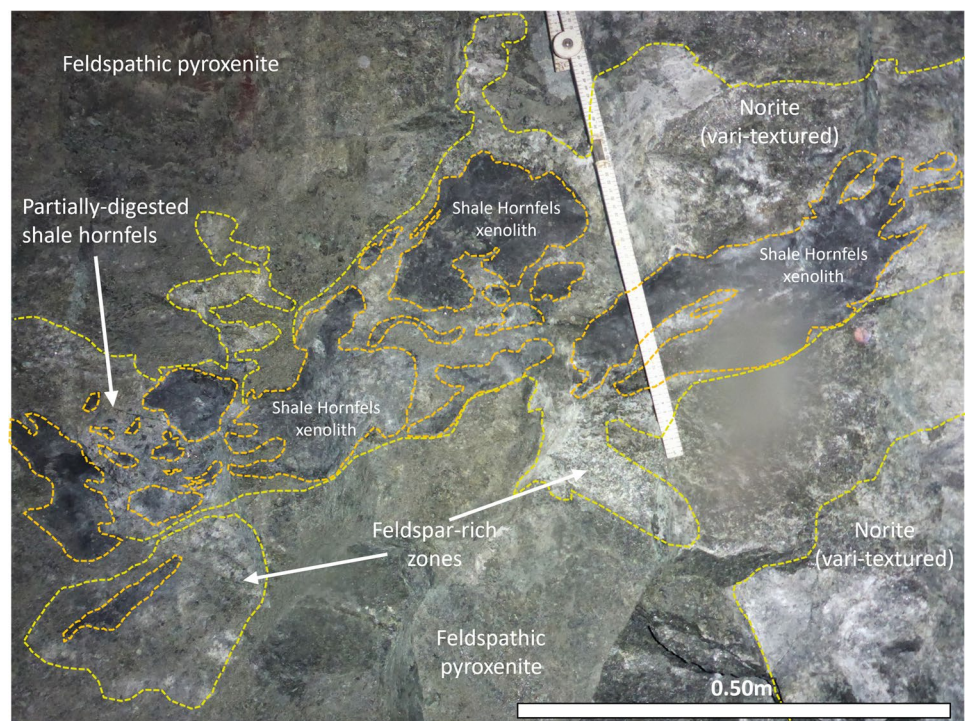
be transitional over zones from tens to hundreds of metres wide. The metasedimentary rocks commonly show bedding and occur mostly in place at their same stratigraphic positions as in the sedimentary rock sequence before intrusion of the Northern Limb, having an open fold structure within the host rocks that predates intrusion (Fig. 2).

The reaction of the magma with different types of sedimentary host rock produced a variety of contact metamorphic and skarn-type rocks (Grobler et al. 2019). Assimilation reactions include metamorphic, metasomatic and melting reactions, dependent on magma-type and host rock, and on PTX conditions within the magma chamber prior to and after intrusion. Typical high-temperature mineral assemblages indicate pyroxene hornfels and granulite facies metamorphic conditions where pyroxene-cordierite hornfels formed after shale, and/or

clinopyroxene-garnet-monticellite calc-silicate formed after dolomite.

Shale metamorphosed to hornfels was preferentially assimilated through melting into the surrounding magmatic units (Fig. 13). In general, hornfels contacts do not appear to be tectonised apart from specific zones of weakness close to major structures that may have accommodated fracturing and shearing along internal bedding planes and along contacts. Metasomatic reactions were locally controlled by calc-silicate hornfels and dolomitic xenoliths within the magma. Volatiles and fluids derived from the xenoliths produced hybrid rock types that range from metamorphic to magmatic in character. Hydrous minerals such as talc-tremolite-serpentine are generally the end-products of alteration fluids which preferentially followed weak zones such as bedding planes within

Fig. 13 The Footwall Assimilation Zone below the reef units of the MCU in Shaft #1 sidewall at 812 m depth. The photo shows the nature and extent of shale hornfels xenoliths remaining after assimilation by the magma. The shale hornfels contributed feldspar and sulfides to the mafic magma as can be observed by the reaction rims around the xenoliths and the coarse sulfide associated with these rims. No cyclical strata are developed, and the dominant magmatic lithology is vari-textured norite



calc-silicate xenoliths and along calc-silicate xenolith-magma contacts. Intense ductile deformation and shearing is commonly associated with calc-silicate xenoliths (Grobler et al. 2019). Alteration and fluid migration was also controlled by structures within the magmatic host rocks, including foliation and intense jointing in association with steep shear zones and thrusts. Low temperature alteration assemblages are associated with fracture zones formed during re-activation of faults and shear zones.

A structural model for the Flatreef

Pre-Bushveld deformation

The TML and similar sub-parallel structures were major pre-Bushveld cratonic features formed in the late Archean during the Limpopo Orogeny (De Wit et al. 1992). Pre-Bushveld NE-SW trending open folding related to the NW-SE-shortening in the D_1 event affected the lower stratigraphic rock units of the Transvaal Supergroup, namely the basal units of the Pretoria Group and the underlying Chuniespoort Group, which are the footwall rocks to the Northern Limb.

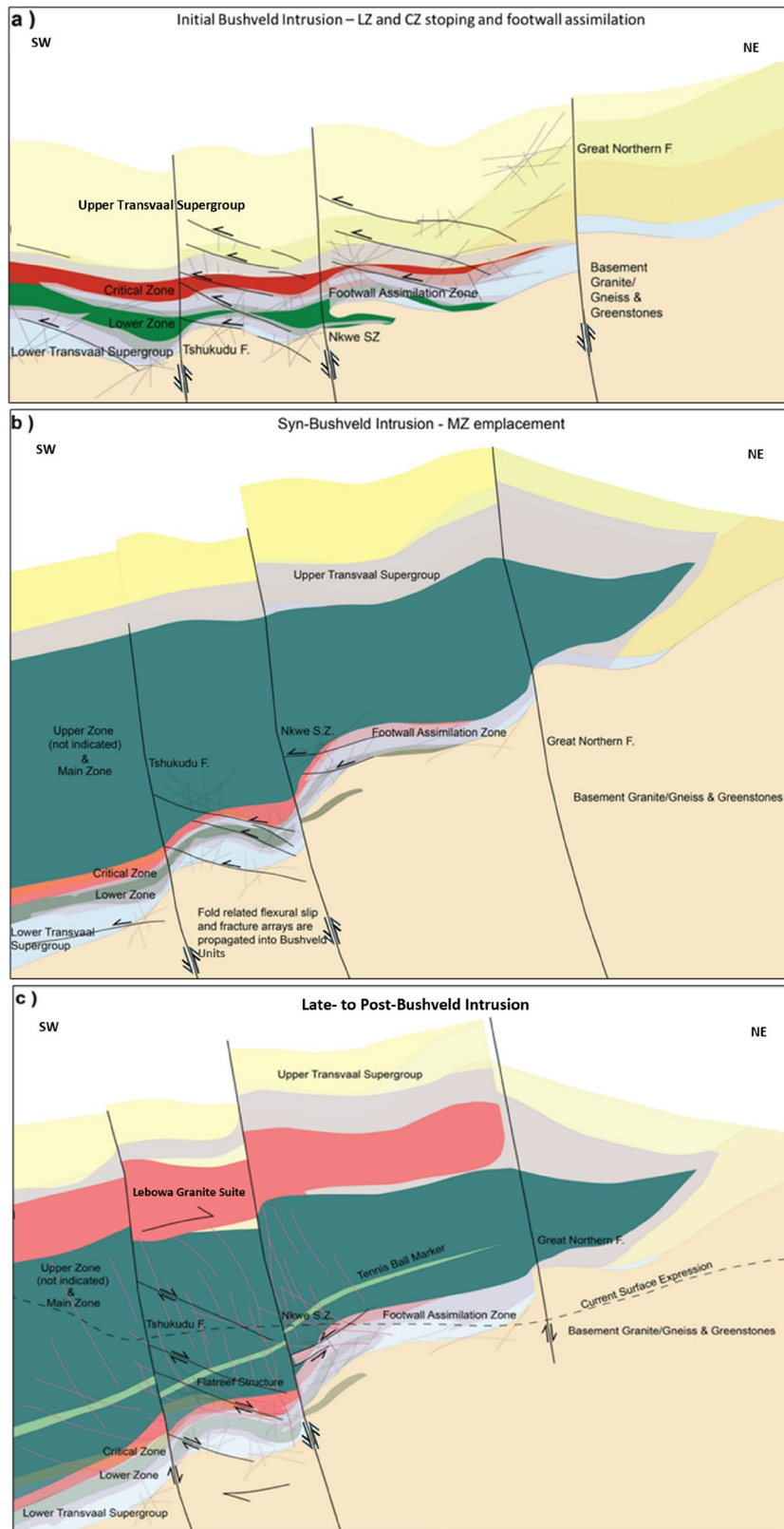
Syn-Bushveld deformation

At the time of Bushveld magmatism, structures such as the TML may have facilitated emplacement of the Bushveld

magmas (Du Plessis and Walraven 1990). Reverse left-lateral movement occurred along the ENE-WSW TML and related faults, such as the Zebediela and the Welgevonden Faults. NE-SW faults, such as the YPF and others may have served as relay structures between the ENE-WSW faults (Basson 2019). The possible northward transgressive intrusion of the Northern Limb (McDonald and Holwell 2011) may have been assisted by the sinistral offset along the NE-SW faults, which may have acted as block faults to elevate lower sedimentary strata increasingly from south to north.

Magma intruded into the undulating footwall sedimentary rocks along bedding planes (Fig. 14a). F_2 folds were superimposed on the NE-trending F_1 open folds. It is possible that the floor of the intrusion formed a dome-and-basin type 1 fold interference pattern at the start of intrusion, if D_2 had already begun at this stage. Undulations in the overlying magmatic units reflect this structure, which weakens upwards through the Critical Zone into the Main Zone. Fault systems developed with a top to the West vergence. These had dominantly reverse separations, but there was layer-parallel extension in places (Figs. 8 and 10). This combination of contraction and extension suggests that the deformation could have been a response by slumping (cf. Maier et al. 2013) to subsidence of the crust as the intrusion thickened.

Melting, devolatilisation and metamorphic processes were governed by a combination of the magma composition and sedimentary rock type. As a result of intrusion, devolatilisation and melting, near in situ remnants of shale hornfels, calc-silicate and occasional metaquartzite xenoliths,



preserving evidence of the open fold geometry of the sedimentary bedding, were incorporated into the magma pile of the Critical and Lower Zones (Fig. 6).

A hiatus between the major influxes of ultramafic (Lower Zone) to mafic (Critical Zone) magma pulses allowed the sedimentary rock in the roof of the Lower Zone magma

Fig. 14 Schematic SW-NE dip sections showing the structural evolution of the Flatreef along the Turfspruit and Macalacaskop strike section. NE trending F_1 folding and NE-trending shear zones are not shown in the schematic sections. **a)** Initial controls on the lower strata, Lower Zone and to a lesser degree, the Critical Zone, intruded into open folded lower Pretoria Group rocks and Chuniespoort Group rocks. NNW-SSE trending shear zones acted as strike-parallel growth faults with downward displacement of the western (down-dip) fault blocks creating space for intrusion and limiting up-dip intrusion from the developing magma chamber. This enhanced the stopping of the Critical Zone intrusion up-dip. **b)** Main Zone emplacement. Main Zone magma causes uplift of the sedimentary roof rocks and thermal erosion of parts of the upper units of the still ductile, consolidating Critical Zone. Magma chamber subsidence causes amplification of the open F_2 folds and causes propagation of the existing reverse fault duplexes through the Lower Zone, Critical Zone, and Main Zone. NNW-SSE shears increase displacement during emplacement and consolidation of the Main Zone due to loading from the magma pile. The Nkwe Shear Zone acts as growth fault with shearing focussed along the upper Critical Zone due to thermal influence and loading from the Main Zone. The reverse to oblique dip-slip shearing causes roll-over folds and monoclinical fold structures within its footwall, thus accommodating the formation of the Flatreef structure with its characteristic locally thickened magmatic strata. **c)** Main Zone consolidation and Upper Zone emplacement stabilised the magma chamber development. The Tennis Ball Marker and associated marker layers differentiate with normal westerly dips and shearing diminishing. During the cooling and subsidence of the Northern Limb, existing NNW-SSE trending steep structures and NNE dipping thrust duplexes were reactivated. The Lebowa Granite Suite intrudes into the metamorphosed sedimentary roof rocks of the Upper Zone and granitic fluids ingress into the extensionally re-activated structures, forming the granite dykes

to react extensively with the cooling magma, causing the subsequent Critical Zone magma influx into already heated and reactive sediments above the preceding pulse. Metamorphism and assimilation decreased until stability was reached within the magma chamber, after which normal fractionation and subsidence ensued during consolidation of the voluminous Main Zone and Upper Zone pulses (Fig. 14b; Walraven and Coertze 1988; Hatton and von Gruenewaldt 1987). This sequence explains the lack of xenoliths within the Merensky Cyclic Unit and lower units of the overlying Bastard Cyclic Unit, as these are found within the Upper Critical Zone of the Flatreef deposit and had limited exposure to the reactive roof above the Lower Zone pulse and the sedimentary rocks forming a temporary roof to the Critical Zone before intrusion of the Main Zone.

Intrusion of the Northern Limb occurred in a locally contractional phase of deformation (D_2), with ENE-WSW shortening as documented by the reverse faults. The intrusion of mafic sills in compressional stress fields has been documented from the Faroe Islands by Walker et al. (2011) and Walker (2016), in the San Rafael sub-volcanic field in Utah (Walker et al. 2017), and in the Loch Scridain Sill Complex, Isle of Mull, UK (Stephens et al. 2017). Despite differences in scale, there is a close analogy between aspects of these studies and the early phases of the Bushveld intrusion:

magma fingers in the Bushveld Complex suggest intrusion in a NNW-SSE direction (Clarke et al. 2009), perpendicular to the ENE shortening, as found in the studies by Walker and co-workers. The Faroes example also has a number of thrust faults within the sill recording the inferred maximum compressional stress; these appear comparable to the reverse faults in the study area.

Reverse displacement along the easterly dipping Nkwe Shear Zone elevated the eastern sedimentary rock block which may have acted as a 'barrier' to intruding magma (Figs. 14b and 11). Magma that did intrude this block interacted with large amounts of sedimentary rock (lower units of the Deutschland, Penge and Malmani Formations). Intrusion of the constrained and steeper part of the developing magma chamber may have prohibited the fractionation of normal magmatic cyclical units east of the Nkwe Shear Zone. This up-dip portion of the Critical Zone does not show the layered strata which developed along the Flatreef (Grobler et al. 2019).

Deformation of semi-consolidated magma by growth faults is suggested by stratigraphic and lithological variability that appear to have been controlled by the major structures such as the Nkwe Shear Zone. Deformation in the Flatreef was accommodated by shearing along the Nkwe Shear Zone. The effect of this was most pronounced within the Upper Critical Zone (Figs. 7 and 11) indicating a period of increased slip on the Nkwe Shear Zone that may have been the result of loading from the intrusion of the overlying Main Zone, concurrent with consolidation in the underlying magmatic units. As a result of reverse displacement along the Nkwe Shear Zone, the Flatreef was displaced downward, thus influencing the ductile, semi-consolidated magma forming the Upper Critical Zone. This zone of magma accumulation formed with its long axis directed NNW-SSE, parallel to the Nkwe Shear Zone, and the NNW-SSE orientated F_2 open fold was amplified. The Upper Critical Zone magma infilled the structure along a strike length of more than 6000 m, locally increasing its thickness (Fig. 11). The Upper Critical Zone, uninfluenced by assimilation of sedimentary rock, formed the magmatic, cyclical units of the Flatreef (Grobler et al. 2019).

The Flatreef attained its monoclinical form, with its gently dipping upper contact at the base of the overlying Main Zone (Fig. 11a). However, the lower contact of the Merensky Cyclic Unit of the Flatreef (Grobler et al. 2019) reflects the local thickening of the stratigraphy due to the infill of semi-consolidated magma within the footwall. Further south along the axis of the Flatreef fold, folds in the Critical Zone which outcrop on the farm Macalacaskop testify to the amplification of the F_2 folding (Figs. 2 and 4).

There is a very rapid upward decrease in displacement along the Nkwe Shear Zone. The displacement gradient of approximately 0.9 is almost an order of magnitude higher

than reverse fault displacement gradients (e.g. Bergen and Shaw 2010), arguing for a decrease in displacement during intrusion. The Main Zone magma influx progressively thickened strata within the F_2 fold, gradually increasing the dip of the magmatic layering of the Main Zone in the Flatreef to the regional dip of the Northern Limb (Fig. 11c). This caused the Tennis Ball Marker Unit to have a constant westerly dip of 20° , in contrast to the generally sub-horizontal dips of the magmatic units of the underlying Flatreef (Fig. 6). Synmagmatic deformation is also recorded at a smaller scale by the shlieren, lenses and drag fold observed in anorthositic units (Fig. 8) and the potholes (Fig. 10).

Late- to post-Bushveld complex deformation

Late- to post-magmatic deformation include features formed due to extensional reactivation of the originally reverse-sense structures such as the reverse faults and steep shear zones (Fig. 14c). Reactivation of these structures was accompanied by intrusion of granitic dykes which were probably part of the Lebowa granite suite, as found in the study area and more extensively along the Northern Limb (Van der Merwe 1976). The Lebowa granitic suite magmas may have evolved in staging chambers beneath the RLS, consistent with their dyke emplacement into the Northern Limb (Skursch et al. 2004). Regional N–S faults, including the Tshukudu Fault, that were present within the basement, Transvaal Supergroup, and RLS of the Northern Limb, experienced normal displacement (east block down) after intrusion of the Bushveld Complex. Dextral displacement along the PSZ also probably postdates the Bushveld Complex intrusion and does not seem to be manifested in the study area.

Conclusions

The geometry and mineral endowment of the Flatreef in the Northern Limb of the Bushveld Complex are strongly controlled by structures. Magmas that formed the Lower Zone intruded along the beds of the Deutschland, Penge and underlying Malmani Formations of the Transvaal Supergroup, which had been folded before intrusion into NE-SW open folds (F_1). Remnant metamorphosed sedimentary rock xenoliths mostly occur within the lower units of the RLS as autochthonous relics of the F_1 open folds.

East-dipping reverse faults and duplexes formed in association with F_2 folding during intrusion. Some of these structures were growth faults. For example, the footwall to the Nkwe Shear Zone was displaced downwards, thereby locally thickening the Upper Critical Zone. Extensional synmagmatic deformation also occurred, for example extending

layers into boudins and forming potholes. The combination of contractional and extensional deformation suggests slumping induced by sagging created by the intrusion.

The combined effect of the F_1 and F_2 folds and the reverse faulting was to impart an undulating, sub-horizontal geometry to the Flatreef. Above the Flatreef, the Main Zone layering is more planar and dips more uniformly at 20° to the west due to the decreasing influence of folding and faulting.

After the emplacement of the RLS, many faults and shear zones were intruded by granitic magmas, probably of the Lebowa granitic suite, and reactivated in extension. Thus, geometry and mineralization of the Flatreef were controlled by the structural evolution of the crust before, during and after intrusion. Its apparently unique geometry in the Bushveld Complex may reflect relatively larger effects of synmagmatic deformation in the study area within the Northern Limb.

Acknowledgements We are grateful for two of the most thorough and constructive reviews that we have ever received from Paul Nex and Ian Basson.

Author contributions Data collection was performed by J. A. N. Brits, D. F. Grobler, and A. Crossingham. A first version of the manuscript was written by J. A.N. Brits. The manuscript was rewritten with additional material by T. G. Blenkinsop and W. Maier. All authors read and approved the final manuscript.

Funding Ivanplats (Pty) Ltd supported the collection of data.

Declarations

Competing Interests The authors have no relevant financial or non-financial interests to disclose.

Open Access This article is licensed under a Creative Commons Attribution 4.0 International License, which permits use, sharing, adaptation, distribution and reproduction in any medium or format, as long as you give appropriate credit to the original author(s) and the source, provide a link to the Creative Commons licence, and indicate if changes were made. The images or other third party material in this article are included in the article's Creative Commons licence, unless indicated otherwise in a credit line to the material. If material is not included in the article's Creative Commons licence and your intended use is not permitted by statutory regulation or exceeds the permitted use, you will need to obtain permission directly from the copyright holder. To view a copy of this licence, visit <http://creativecommons.org/licenses/by/4.0/>.

References

- Anhaeusser CR, Wilson JF (1981) The Granitic-gneiss Greenstone Shield. *Develop Precambrian Geol* 2:423–499
- Armitage PEB (2011) Development of the Flatreef in the northern limb of the Bushveld Complex at Sandsloot, Mokopane District, South Africa PhD Thesis, University of Greenwich
- Basson IJ (2019) Cumulative deformation and original geometry of the Bushveld Complex. *Tectonophysics* 750:177–202

- Bergen KJ, Shaw JH (2010) Displacement profiles and displacement-length scaling relationships of thrust faults constrained by seismic-reflection data. *Bull Geol Soc Am* 122:1209–1219. <https://doi.org/10.1130/B26373.1>
- Brandl G, Reinold WU (1990) The structural setting and deformation associated with the pseudotachylite occurrences in the Palala Shear Belt and Sand River Gneiss, Northern Transvaal. *Tectonophysics* 171:201–220
- Bumby AJ, van der Merwe R (2004) The Limpopo Belt of southern Africa: an overview. *Tempos and events in precambrian time*. Elsevier, Amsterdam, pp 217–222
- Carr HW, Groves DI, Cawthorne RG (1994) The importance of syn-magmatic deformation in the formation of Merensky Reef pot-holes in the Bushveld Complex, Scientific communications. *Econ Geol* 89:1398–1410
- Clarke BM, Uken R, Watkeys MK (2000) Intrusion mechanisms of the southwestern Rustenburg Layered suite as deduced from the Spruitfontein inlier. *S Af J Geol* 103:120–127
- Clarke BM, Uken R, Watkeys MK, Reinhardt J (2005) Folding of the Rustenburg layered suite adjacent to the Steelpoort pericline: implications for syn-bushveld tectonism in the eastern Bushveld Complex. *S Af J Geol* 108:397–412
- Clarke B, Uken R, Reinhardt J (2009) Structural and compositional constraints on the emplacement of the Bushveld Complex, South Africa. *Lithos* 111:21–36. <https://doi.org/10.1016/j.lithos.2008.11.006>
- De Wit MJ, Jones MG, Buchanan DL (1992) The geology and tectonic evolution of the Pietersburg Greenstone Belt, South Africa. *Precamb Res* 55:123–153
- Du Plessis CP (1987) New perspectives on early Waterberg Group sedimentation from the Gatkop area, northwestern Transvaal. *S Afr J Geol* 90:395–408
- Du Plessis CP, Walraven F (1990) The tectonic setting of the Bushveld Complex in Southern Africa, Part 1. *Tectonophysics* 179:305–319
- Structural deformation and distribution
- Eriksson PG, Reczko BFF (1995) The Sedimentary and Tectonic setting of the Transvaal Supergroup Floor Rocks to the Bushveld Complex. *J Af Earth Sci* 21:487–504
- Friese A, Chunnet G (2004) Tectono-magmatic development of the northern limb of the Bushveld Igneous Complex, with special reference to the mining area of Potgietersrus Platinums Limited, Geoscience Africa 2004 Abstract Volume, University of the Witwatersrand, Johannesburg, South Africa, pp 209–10
- Friese AEW (2003) Bushveld Igneous Complex: Origin and plate tectonic setting within the context of the geodynamic evolution of southern Africa during the late Palaeoproterozoic. *Extended Abstracts, Symposium on Structural Geology of the Bushveld Complex*, Geol. Soc. S.A
- Friese AEW (2012) Interpretation of the tectono-structural setting and evolution and assessment of the structural geology and its impact on mining of mine 1 area, Platreef Project, Northern Bushveld Complex, Mokopane, South Africa. *Terra Explora Consulting Report*. 2012/4
- Geological Survey of South Africa (1978) 2428 Nylstroom 1:250 000. *Geological Map Series*
- Good N, De Wit MJ (1997) The Thabazimbi-Murchison Lineament of the Kaapvaal Craton, South Africa \pm 2700 ma of episodic deformation. *J Geol Soc Lond* 154:93–97
- Grobler DF, Brits J, Maier WD, Crossingham A (2019) Litho- and chemostratigraphy of the Flatreef PGE deposit, northern Bushveld Complex. *Min Depos* 54:3–28
- Hatton CJ, Von Gruenewaldt G (1987) The Geological Setting and Petrogenesis of the Bushveld Chromitite Layers. In: Stowe CW (eds.). *Evolution of chromium ore fields*. 109–143
- Holwell DA, Jordaan A (2006) Three-dimensional mapping of the platreef at the Zwartfontein South mine: implications for the timing of magmatic events in the northern limb of the Bushveld Complex, South Africa. *Appl Earth Sci* 115:41–48
- Holzer L, Frei R, Barton JM Jr., Kramers JD (1998) Unravelling the record of successive high grade events in the Central Zone of the Limpopo Belt using Pb single phase dating of metamorphic minerals. *Precamb Res* 87:98–115
- Kekana SM (2014) An investigation of mineralization controls in the upper section of the Platreef in the southern sector, on Turfspruit, Northern Limb. MSc thesis, University of the Witwatersrand. pp 143
- Kinnaird JA, McDonald I (2005) An introduction to Mineralisation in the Northern Limb of the Bushveld Complex. *Appl Earth Sci Trans Inst Min Metall B* 114:B194–B198
- Kinnaird JA, Hutchinson D, Schurmann L, Nex PAM, de Lange R (2005) Petrology and Mineralization of the Southern Platreef: Northern limb of the Bushveld Complex, South Africa. *Mineral Deposita* 40:576–597
- Kinnaird JA, Yudovskaya MA, McCreesh M, Huthmann FM, Botha TJ (2017) The Waterberg Platinum Group Element Deposit: atypical mineralisation in mafic-ultramafic rocks of the Bushveld Complex, South Africa. *Econ Geol* 112:1367–1394
- Lea SD (1996) The geology of the Upper critical zone, northeastern Bushveld Complex. *S Afr J Geol* 99(3):263–283
- Liang C, Liu X, Kramers JD, Zheng C, Hu P, Zhang Q (2021) Deformation characteristics, kinematic analysis, and formation ages of gneissose palala granite in the Palala Shear Zone, southern boundary of the Central Zone, Limpopo Belt, South Africa. *J Af Earth Sci* 175:104092
- Maier WD, De Klerk L, Blaine J, Manyeruke T, Barnes SJ, Stevens MVA and Mavrogenes JA (2008) Petrogenesis of contact-style PGE mineralization in the northern lobe of the Bushveld Complex: comparison of data from the farms Rooipoort, Townlands, Drenthe and Nonnenwerth. *Mineralium Deposita*, 43, pp.255-280.
- Maier WD, Barnes SJ, Groves DI (2013) The Bushveld Complex, South Africa: formation of Platinum-Palladium, chrome- and vanadium-rich layers via hydrodynamic sorting of a mobilized Cumulate Slurry in a large, relatively slowly cooling. *Subsiding Magma Chamb Mineral Deposita* 48:1–56
- Maier WD, Abernethy KEL, Grobler DF, Moorhead G (2021) Formation of the Flatreef deposit, northern Bushveld, by hydrodynamic and hydromagmatic processes. *Mineral Deposita* 56:11–30. <https://doi.org/10.1007/s00126-020-00987-5>
- Maier WD, Barnes SJ, Godel BM, Grobler D, Smith WD (2023) Petrogenesis of thick, high-grade PGE mineralisation in the Flatreef, northern Bushveld Complex. *Mineral Deposita* 58:881–902
- McCourt S, Vearncombe JR (1987) Shear zones bounding the Central Zone of the Limpopo Mobile Belt, Southern Africa. *J Struct Geol* 9:127–137
- McCourt S, Vearncombe JR (1992) Shear zones of the Limpopo Belt and adjacent granitoid-greenstone terrains: implications for late archaean crustal evolution in southern Africa. *Precambrian Res* 55:553–570
- McDonald I, Holwell DA (2011) Geology of the Northern Bushveld Complex and the setting and Genesis of the Platreef Ni-Cu-PGE deposit. *Econ Geol* 17:297–327
- McDonald I, Holwell DA, Armitage PEB (2005) Geochemistry and mineralogy of the platreef and critical zone of the northern lobe of the Bushveld Complex, South Africa: implications for Bushveld stratigraphy and the development of PGE mineralisation. *Mineral Deposita* 40:526–549. <https://doi.org/10.1007/s00126-005-0018-6>
- Meinster B (1974) Thrusting and block-faulting around Gatkop east of Thabazimbi. *Transvaal. Annals Geol Surv S Afr* 10:57–72

- Mudd GM, Jowitt SM, Werner TT (2018) Global platinum group element resources, reserves and mining—A critical assessment. *Sci Total Environ* 622:614–625
- van der Merwe MJ (1976) The layered sequence of the Potgietersrus Limb of the Bushveld Complex. *Econ Geol* 71:1337–1351
- Van der Merwe MJ (1978) The geology of the basic and ultramafic rocks of the Potgietersrus limb of the Bushveld Complex. Thesis, University of the Witwatersrand
- Naldrett AJ, Gasparrini EC, Barnes SJ, Von Gruenewaldt G, Sharpe MR (1986) The Upper critical zone of the Bushveld Complex and the origin of Merensky-type ores. *Econ Geol* 81:1105–1117
- Nell J (1985) The Bushveld metamorphic aureole in the Potgietersrus area; evidence for a two-stage metamorphic event. *Econ Geol* 80:1129–1152
- Nex PAM (2005) The structural setting of mineralisation on Tweefontein Hill, Northern Limb of the Bushveld Complex, South Africa. *Appl Earth Sci* 114:243–251
- Peters BF, Parker HM, Joughin W, Treen J, Coerzee V, Marais F (2017) Platreef Project, Platreef 2017 Feasibility Study, Ivanhoe Mines, publ. on <https://www.sedar.com>
- Saumur BM, Cruden AR (2017) Ingress of magmatic Ni-Cu sulphide liquid into surrounding brittle rocks: Physical & structural controls. *Ore Geol Reviews* 90:439–445. <https://doi.org/10.1016/j.oregeorev.2017.06.009>
- Schaller M, Steiner O, Studer I, Holzer L, Herwegh M, Kramers JD (1999) Exhumation of Limpopo Central Zone granulites and dextral continent-scale transcurrent movement at 2.0 Ga along the Palala Shear Zone, Northern Province, South Africa. *Precamb Res* 96:263–288
- Stephens L, Walker RJ, Healy D, Bubeck A, England RJ, McCaffrey KJW (2017) Igneous sills record far-field and near-field stress interactions during volcano construction: Isle of Mull, Scotland. *Earth Planet Sci Lett* 478:159–174. <https://doi.org/10.1016/j.epsl.2017.09.003>
- Vermaak CF (1976) The Merensky reef: thoughts on its environment and genesis. *Econ Geol* 71:1270–1298
- Walker RJ (2016) Controls on transgressive sill growth. *Geology* 44:99–102. <https://doi.org/10.1130/G37144.1>
- Walker RJ, Holdsworth RE, Imber J, Ellis D (2011) Onshore evidence for progressive changes in rifting directions during continental break-up in the NE Atlantic. *J Geol Soc Lond* 168:27–48. <https://doi.org/10.1144/0016-76492010-021>
- Walker RJ, Healy D, Kawanzaruwa TM, Wright KA, England RW, McCaffrey KJW, Bubeck AA, Stephens TL, Farrell NJC, Blenkinsop TG (2017) Igneous sills as a record of horizontal shortening: the San Rafael subvolcanic field, Utah. *GSA Bull* 129:1052–1070. <https://doi.org/10.1130/B31671.1>
- Walraven F, Coertze FJ (eds) (1988) Ext. Abstr. Geocongress '8, 22nd Earth Science Congress. Ext. Abstr. Geocongress '8, 22nd Earth Science Congress, Geol. Soc. S. Afr., Durban, pp 705–708
- Willemsse J (1969) The geology of the Bushveld Igneous Complex, the largest repository of magmatic ore deposits in the world. *Econ Geol Monogr* 4:1–22

Publisher's Note Springer Nature remains neutral with regard to jurisdictional claims in published maps and institutional affiliations.